Sustainability of Aluminum-based alloys in Chloride Ions Containing Environment

Ravijot Singh[a], Saurabh Sharma[b], Sangamdeep Singh[b]

[a]*M.Tech Scholar, Department of Mechanical Engineering, Sri Sai College of Engineering & Technology, Badhani*

[b]*Assistant Professor, Department of Mechanical Engineering, Sri Sai College of Engineering & Technology, Badhani*

Abstract : The aluminium element is considered a highly corrosion resistant element, due to which it is worthy to investigate the Al-based alloys against different corrosion mediums such as NaCl, H_2SO_4, HNO_3 etc.. The Al-based alloys are also preferred due to their light weight. Presently, the alloys were prepared using melting and casting route in an inert environment. All the Al-based alloys were characterized using X-ray diffraction, differential scanning calorimetry (DSC) and optical microscopy. The XRD tests were conducted to analyze their phase formation and DSC was used to estimate the melting point of all the alloys. the surface properties such as hardness values and micrographs were also taken. The hardness testing apparatus was used for determining the hardness value, after which the graph was plotted to observe the effect of composition. Finally, the corrosion resistance of all of the produced alloys in 3.5 weight percent NaCl solution was analyzed. It was also possible to compare the corrosion parameters of all of the different alloys. The corrosion current density (i_{corr}), corrosion potential (E_{corr}), and corrosion rate are the three primary corrosion parameters investigated in this work.

Keywords: Brazing filler, X-ray diffraction, Optical microscopy, Differential scanning calorimetry, Corrosion

1. Introduction:

Manufacturers of thermoelectric devices state that brazing is the most often used technique of attaching components in thermoelectric devices. This flexible metal joining process connects two (or more) components together by employing a filler metal as an adhesive and connecting them with a brazing rod (an alloy with a lower liquidus temperature than either component it is used to join). Brazing is a process in which an assembly of components and filler metals is heated to a temperature above the liquidus temperature of the filler metal (for brazing, a minimum liquidus temperature of 450°C is required in order to distinguish the process from soldering, which uses fillers with a liquidus temperature below 450°C), at which point the filler metal melts and turns molten [1-4].

Recently, various research initiatives set the objective to prevent, respectively limit intermetallic phase formation by utilizing high entropy filler materials [5,6]. In earlier investigations, high entropy filler metals were employed in order to effectively combine nickel-based super alloys as well as SOFCs [7, 8]. Based on the high entropy notion, metallic multi-component alloys with an equal distribution of their alloy components are able to minimize the number of potential occurring phases by generating a random solid solution structure [9,10]. According to Yeh et al., a high entropy value encourages the creation of a random solid solution (RSS), in which the alloy components are randomly dispersed across its lattice.

Specifically, the equimolar high entropy alloy Al-Si-Sn-Zn-Cu was investigated as a filler material for the vacuum brazing procedure used to link the Al-based super alloy. It is worth noting that the liquidus temperature of Al-Si-Sn-Zn-Cu is 1346 degrees Celsius, which is much higher than the solutioning temperature of Mar-M 247, which varies between 1080 and 1170 degrees Celsius [11]. It has been chosen to alloy the Al-12Si alloy in order to lower the melting point of the brazing filler, which will be validated using DSC data. Following that, an electrochemical potentiostat was used to examine the corrosion resistance of all of the produced alloys in 3.5 weight percent NaCl. It was also possible to compare the corrosion parameters of all of the different alloys.

Figure 1 Various Classes of HEAs as Brazing Filler

Material and Methods:

2.1. Materials: The physical characteristics of the as-received powders of aluminum, copper, cobalt, molybdenum, silicon, tin, copper, and zinc employed in this investigation were used to synthesize the samples. The as-received Al, Co, Mo, Si, Sn, Zn, and Cu powders were weighed according to the required compositions (Table 1).
Table 1 Composition of alloys (wt.%)

Compositions	Co	Mo	Si	Sn	Zn	Cu	Al
C_0	0.5	0.5	12	0	0	0	Balance
C_1	0.5	0.5	12	0.75	0.75	2	Balance
C_2	0.5	0.5	12	0.75	0.75	4	Balance
C_3	0.5	0.5	12	0.75	0.75	6	Balance
C_4	0.5	0.5	12	0.75	0.75	10	Balance

First and foremost, the powders were taken and combined into the mortar in accordance with the compositions. Then, using a 15 mm diameter die mounted in uni-axial compaction machinery, the powders were compacted to produce the final product. The pellets were made in this manner and were of five distinct compositions. In the next step, the pellets were inserted into the copper mold, and the requisite vacuum level was obtained, after which inert argon gas was purged from the copper mold. Finally, the pellets were melted five times with a spark, the strength of which may be controlled by varying the current flow rate in the circuit. By impacting electrons with a large amount of kinetic energy, the temperature of the material will rise very quickly very quickly.

2.2. Methods
Extensive phase investigation of aluminum-based alloy samples was carried out using XRD, which operates on the basis of Bragg's Law. Equipment using Cu radiation was used to conduct XRD experiments on a variety of various compositions. The analysis was carried out in the 2 theta range of 20^o-80^o. All XRD peaks were fitted using peak fitting to get the peak locations and full width at half maxima, which were then computed. Differential Scanning is a kind of scanning in which two or more images are compared side by side. For thermal examination of materials in which phase transitions such as melting, glass transitions, or exothermic decompositions are investigated, the calorimetry method is utilized. Both the reference sample and

the sample on which thermal analysis is to be performed are necessary for this experiment to be completed. The reference sample should have a well-defined heat capacity across the temperature range that will be scanned in order to be useful.
For the optical microscopy, the sample were polished with SiC abrasive papers, after which polishing was done using velvet cloth having alumina suspension diluted with water on a double disk polishing machine. For the hardness of the samples, the Vickers hardness tester was used. The 5 hardness values were taken, after which the average was calculated. The corrosion tests, the tests were carried out three times on each sample repeatedly in NaCl. The experiment began with the plot of the OCP (Open circuit potential), and after a stable condition had been attained, the polarization curves were constructed using the data from the plot. The values of E_{corr} and i_{corr} were found after fitting the curves.

3. Results and Discussions

3.1. X-Ray Diffraction of Al-based alloys

We performed XRD analysis on each and every one of the aluminum-based alloys and tested in order to determine which phases were present in the alloys. Figure 2 shows crystalline peaks of two separate phases of aluminum and silicon that may be distinguished. According to certain theories, the strength of the Si peak has been weakening as a consequence of the creation of supersaturated Si solutions in the Al, as well as the rapid cooling rates that were seen throughout the melting and casting processes. Because the alloying elements Co, Mo, Sn, Zn, and Cu were completely dissolved and a solid solution produced, it is not feasible to observe peaks for these elements in the resulting analysis in figure 2 of C_1. When comparing the other alloying elements, including alloys, to the single Si-containing alloy, the intensity of the Al and Si peaks in the other alloying elements, including alloys, is substantially decreased in comparison to the single Si-containing alloy (C_0).

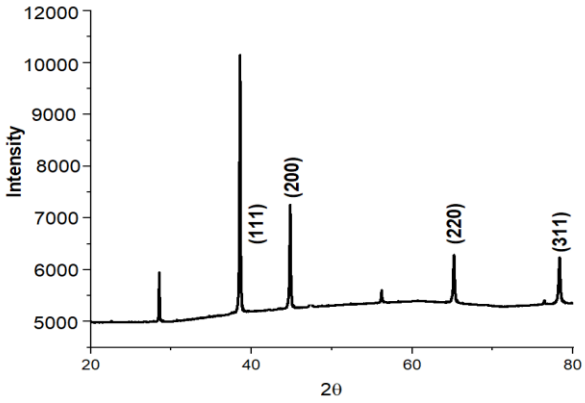

Figure 2. XRD pattern of C_0 alloy

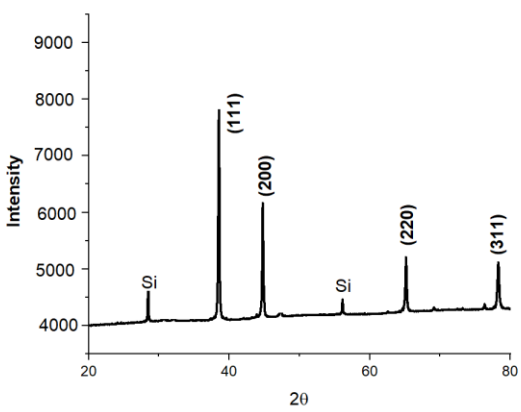

Figure3. XRD pattern of C_1 sample

3.2. XRD peak shift Analysis

This migration of the most prominent XRD peak of alloys from its original location to its left side indicates that the lattice expansion of Al atoms has happened as a consequence of solid solution formation with alloying elements (Co, Mo, Cu, Sn, Zn, Si). As the concentration of Cu in the solution rose, the lattice structure continued to grow as seen in figure 4.

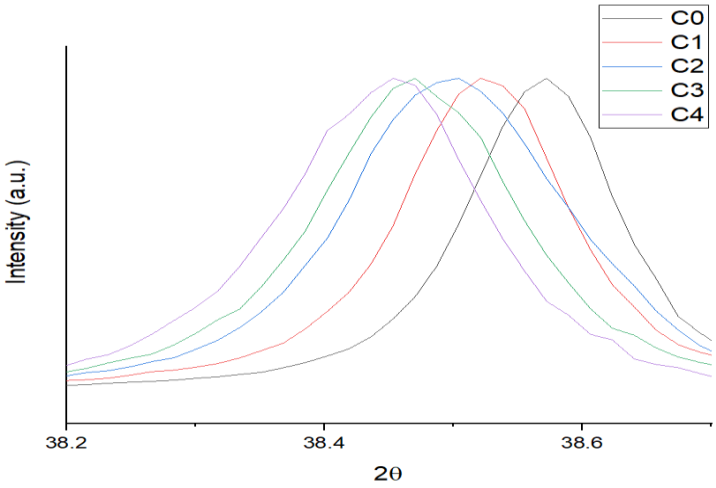

Figure 4. The Prominent XRD peak shift of Al-based alloys

3.3. DSC and Optical Microscopy

The DSC study was carried out on all of the Al-based alloys that are presently being synthesized. All alloys were submitted to DSC testing up to 700 degrees Celsius. According to research, 590.6 degrees Celsius was revealed to be the melting point of C_0 alloy. The melting point of the alloys decreased when alloying was introduced. Furthermore, when the Cu concentration grew, the melting point decreased. Because filler materials should have the lowest melting point possible, it means that the Cu addition makes the alloy more suitable for use as a filler. The optical micrographs of all the alloys are shown in Figure 6.

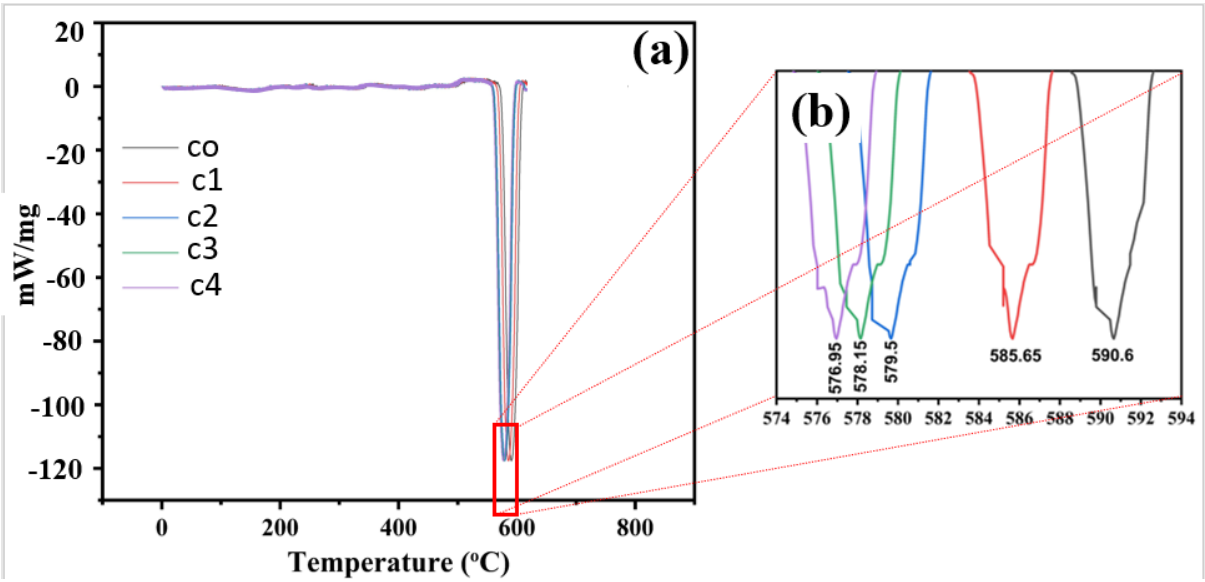

Figure 5.DSC of Al-based alloys

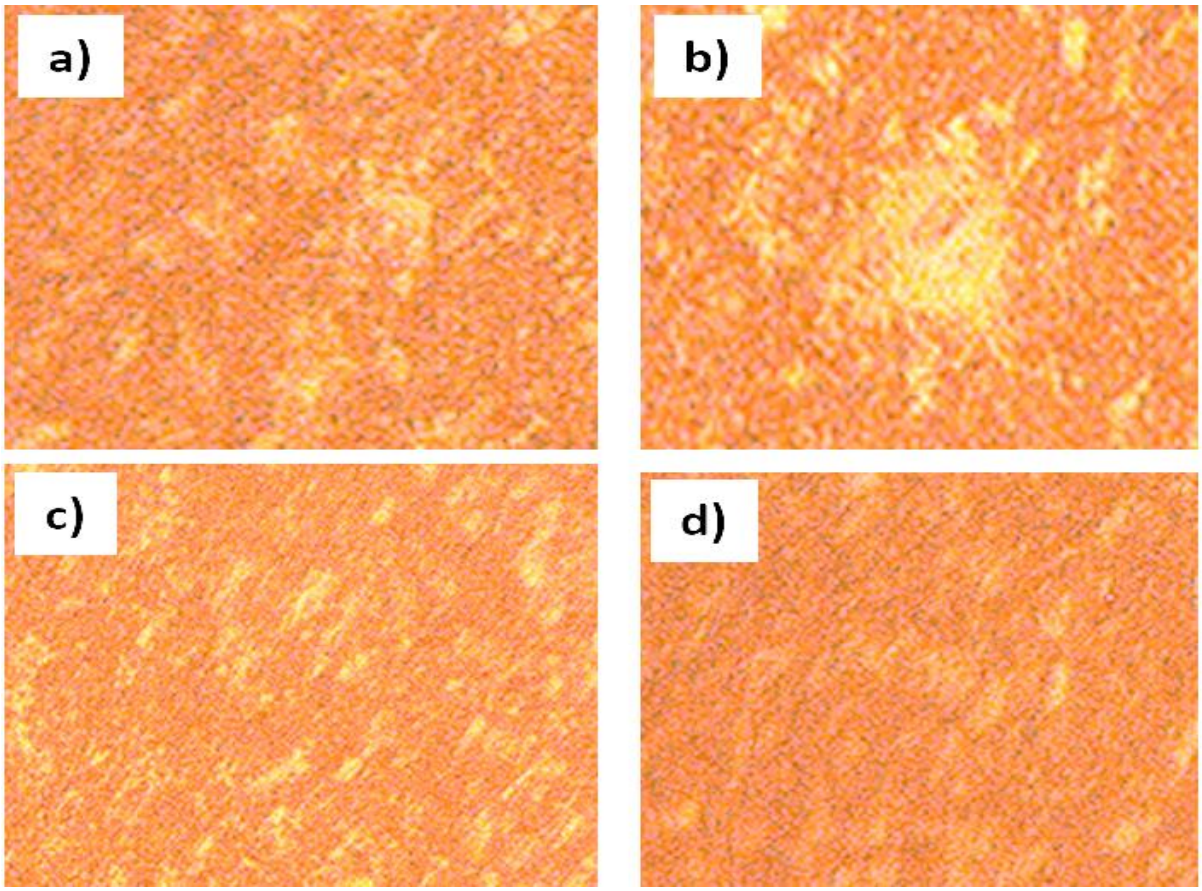

Figure 6 Optical micrographs of a) C1, b) C2, c) C3, and d) C4

3.4. Electrochemical analysis of Al-based alloys in 3.5% NaCl solution

After the polished samples of aluminum-based alloys were linked with copper wire and subsequently mounted in epoxy resin, just one surface with a surface area of one centimeter square (cm^2) was subjected to corrosive conditions. The sample was used as the working electrode, and it was placed in a three-electrode glass cell with a counter electrode (platinum mesh) and a reference electrode to conduct the experiment (SCE). Each experiment started with an hour of ocp (open circuit potential) to allow the sample to stabilize. The potentiodynamic polarizaton curve was then generated by scanning the electrodes at a rate of 0.5 mV/s. Using the tafel fit, it was possible to determine the electrochemical parameters of the sample, such as the corrosion potential (Ecorr) and the corrosion current density (icorr). Because the corrosion rate (CR) is closely related to the corrosion current density (i_{corr}), the value of i_{corr} was used to compute the corrosion rate (CR). In order to compute CR, it was required to take into account two more factors: density and equivalent weight. Figure 7 shows the potentiodynamic polarization curves of all of the alloys, which were created in a 3.5 weight percent NaCl solution in order to highlight the influence of Cu on corrosion behavior. The drop in corrosion potential implies a decrease in the susceptibility to corrode, and the decrease in current density indicates a decrease in the rate of corrosion. The electrochemical corrosion parameters are listed in Table 2.

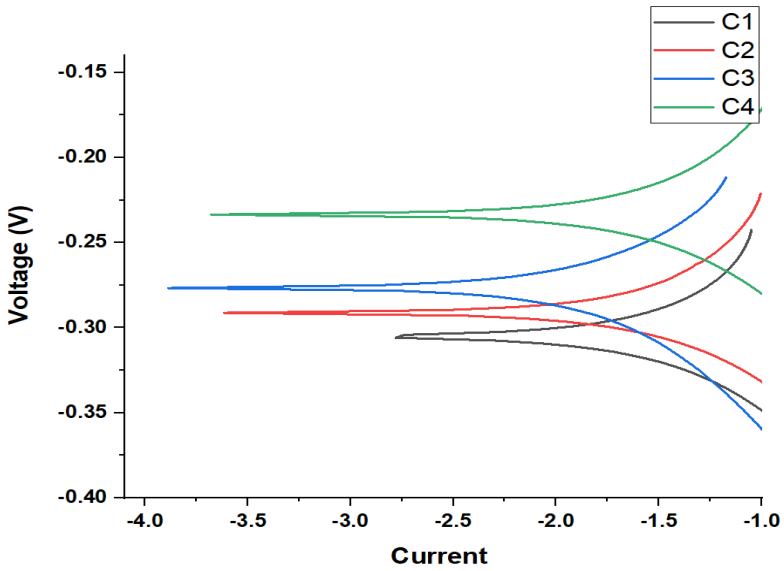

Figure 7. Potentiodynamic polarization curves of samples in 3.5 wt% NaCl aqueous solution

Table 2 Potentiodynamic polarization results of samples in 3.5 wt % NaCl aqueous solutions

Alloy	E_{corr} (mV)	i_{corr} ($\mu A/cm^2$)	Corrosion rate (mmpy)
C1	-305.66	38676.80	365.7055
C2	-290.33	36575.32	345.8351
C3	-270.80	22330.34	211.1428
C4	-234.85	47467.45	448.8248

Conclusion: The Al-based alloys were successfully synthesized using melting and casting technique. The melting point of Al-based alloy decreased with the addition of alloying elements and further with the increase of Cu content. But the significant melting temperature drop was there up to certain increase of Cu%. The density of alloys increased with increase of Cu content. In addition, the actual density was slightly lesser comparing with the theoretical density due to presence of some porosity. The hardness of Al-based alloys increased with the increase of Cu wt %. The corrosion performance was superior in C_3 alloy in 3.5% NaCl than other investigated alloys in this study.

Conflict of Interest: Authors declare no conflict of interest.

References:

1. T. Onzawa, A. Suzumura, and M. Ko, "Brazing of titanium using low-melting-point Ti-based filler metals," Welding Journal, vol. 462, 1990.
2. A. E. Shapiro and Y. A. Flom, "Brazing of titanium at temperatures below 800°C: review and prospective applications," DVS Berichte, vol. 243, p. 254, 2007.
3. B.S. Murty, J.W. Yeh,.; S. Ranganathan,"High. Entropy Alloys, 1st ed."; Butterworth-Heinemann: London, UK, 2014.
4. M. Way, J. Willingham, R. Goodall, Brazing filler metals, Int. Mater. Rev. 0 (2019) 1–29. https://doi.org/10.1080/09506608.2019.1613311
5. Tillmann W, Wojarski L, Manka M et al. (2018) Eutectic high entropy alloys—a novel class of materials for brazing applications, Proceedings from the International Brazing & Soldering Conference, 15th to 18th April 2018, New Orleans, pp 142–148
6. Hardwick L, Rodgers P, Pickering EJ et al. (2019) Development of novel nickel-based brazing alloys, utilising alternative melting point depressants and high entropy alloy concepts, Proceedings from Brazing, high temperature brazing and diffusion bonding, 12th International Conference, 21st to 23rd May 2019, Aachen, pp 7–17
7. Tillmann W, Wojarski L, Ulitzka T et al. (2019) Brazing of high temperature materials using melting range optimized filler metals based, Proceedings from Brazing, high temperature brazing and diffusion bonding, 12th International Conference, 21st to 23rd May 2019, Aachen, pp 1–6
8. Cantor B, Chang ITH, Knight P et al (2004) Microstructural development in equiatomic multicomponent alloys. Mater Sci Eng A 375-377:213–218. https://doi.org/10.1016/j.msea.2003.10.257
9. Zhang LX, Shi JM, Li HW et al (2016) Interfacial microstructure and mechanical properties of ZrB 2 SiC C ceramic and GH99 superalloy joints brazed with a Ti-modified FeCoNiCrCu high-entropy alloy. Mater Des 97:230–238. https://doi.org/10.1016/j.matdes. 2016.02.055
10. Yeh J-W (2013) Alloy design strategies and future trends in highentropy alloys. JOM 65(12):1759–1771. https://doi.org/10.1007/s11837-013-0761-6
11. Baldan R, da Rocha RLP, Tomasiello RB et al (2013) Solutioning and aging of MAR-M247 nickel-based superalloy. J Mater Eng Perform 22(9):2574–2579.